

Reconstruction of 1650 BC Fragmented Wall Paintings by Exploitation of the Thematic Content

D. Fragoulis¹, C. Papaodysseus¹, A. Skembris^{1*}, P. Rousopoulos¹, M. Panagopoulos¹, Th. Panagopoulos¹, C. Triantrafyllou¹.

1. School of Electrical and Computer Engineering, National Technical University of Athens, 9 Heroon Polytechniou, GR-15773, Athens, GREECE.

*Corresponding author, email:saverios@mail.ntua.gr

Permission to publish this Abstract separately is granted.

Abstract—In this paper two approaches of general applicability for placing fragments of important archeological objects in their proper position are presented. Both methods are based on the thematic content of the drawings depicted on fragments of 1650 B.C. wall-paintings, excavated at the Greek island of Thera. The first method employs the statistical nature of the drawn figures' dimensions and gives an estimate of the probability that two fragments belong to the same decorative element and are properly placed in it. During the second method, the authors first prove that there are certain contour lines of the drawn objects that correspond to specific geometric archetypes. Subsequently, an exhaustive Least Squares novel approach is applied in order to correctly place fragments containing broken contour lines of the same decorative element onto their proper geometric archetype. Both methods have been quite successfully applied to the reconstruction of various fragmented wall-paintings.

Index Terms— Image line pattern analysis, archaeological image edge analysis, archaeological object reconstruction, curve fitting, statistical pattern matching.

I. INTRODUCTION – PROBLEM DESCRIPTION

THE discovery of wall paintings at Akrotiri of the Greek island Thera (Santorini), is of outstanding importance for human knowledge of the early Aegean world and not only. According to prominent archaeologists, these wall-paintings rank alongside the greatest archaeological discoveries. Extensive archaeological research over the past 35 years has shown that before the catastrophic eruption of the Thera volcano, in c. 1650 B.C., Akrotiri suffered a major disaster due to earthquakes [1]. The tremendous earthquake caused the collapse of the underlying walls and wall-paintings, but the succeeding eruption was the major factor for their excellent preservation. The good condition of the fragments allows archaeologists to reconstruct wall paintings, which are usually scattered into many hundreds, or even thousands, of fragments mixed with the fragments of other wall paintings. The restoration of the wall paintings from the fragments is a very painstaking and time consuming process, frequently demanding many months or even years of dedicated, experienced personnel work for a single wall painting restoration.

In this paper, we present two methodologies for reconstructing wall-paintings on the basis of the thematic content of their constituent fragments. Apart from aiding the reconstruction process, the approaches introduced here may accomplish fragment matching, even in cases where human experts are intrinsically unable to do so, as it will become evident in the subsequent analysis. Both approaches take advantage of the fact that the artist(s) had, most probably, the intention of drawing repeated geometric patterns. We stress that such drawing techniques seem to be essentially novel for the considered era of Late Bronze Age, c. 1650. In each of the two approaches presented here, the properties of the appropriate geometric shape of the depicted figure are quantified and used in order to statistically verify a potential match between two fragments, or in order to properly position two pieces that contain part of the same prototype but do not necessarily come in direct contact with each other. For the first approach, we use statistical methods, whereas for the second approach we have developed a method of exhaustive Least Squares curve fitting.

The contribution of the present paper to this problem of automatic reconstruction of wall-paintings is in the fields of pattern identification and matching, as well as curve fitting. This is a field where quite extensive research has been done the last decades (e.g. [2] - [9]).

II. USE OF STATISTICAL METHODS FOR MATCHING A LARGE CLASS OF FRAGMENTS

In this section, a method for matching a large class of fragments with a specific type of content will be presented. We would like to point out that this approach has very little to do, if at all, with 2D or 3D puzzle solving and/or broken object reconstruction based on contour matching (e.g. [10]-[14]). This is so, because for applying the introduced method no need for contact between matching

fragments is required; in effect, the power of this approach lies mainly in the fact that it can be applied in cases where intermediate material between the fragments to be matched is missing. In this case, the dedicated reconstruction personnel has great difficulty in reconstructing the wall painting, since they rely on verification of adjacent fragments' "dovetail" contact.

A. A first stage processing

It seems that a major decorative element in most wall-paintings of the third floor of the house called 'Xeste 3', consists of alternating black and blue stripes, like the ones shown in Fig. 1. As a consequence, hundreds of fragments depicting parts of these decorative elements have been found so far. We frequently refer to these fragments with the name Black-Blue-Stripe (BBS) fragments. The restoration of the wall-painting parts consisting of these fragments is a serious problem, which, frequently, the human experts have substantial difficulty to solve, especially when no contact between neighboring fragments exists. In this section, we give a mathematical solution to this problem by exploiting the facts that:

- a) It seems the artist(s) had the intention to draw parallel BBS.
- b) The BBS' width varies erratically, probably due to inaccuracies and imperfections in the drawing process.

1) Parallel line grid extraction

For the subsequent analysis, it is essential to obtain an as accurate as possible representation of the black stripes' edges. To achieve this, various image segmentation methods have been examined and applied (e.g. [15] – [17]). We would like to point out that the authors have developed a segmentation method, which is specifically tailored to this problem's needs and offers really satisfactory results [18]. After the applied image segmentation, we enumerate the black stripes and their boundaries starting from one having all other boundaries in its same side. In this way, the chains of pixels B_1 and B_2 constitute the first and the second boundary of the first black stripe, B_3 and B_4 constitute the first and the second boundary of the second black stripe, etc. Next, in each such fragment, we determine the parallel line grid that best fits the whole ensemble of black stripe boundaries. In other words, we determine the class of parallel lines $y = ax + b_i$, where $y = ax + b_1$ best fits the first boundary while simultaneously $y = ax + b_2$ best fits the second boundary B_2 , etc, all in the Least Squares sense. Analytically, if $(x_{j,i}, y_{j,i})$ are the coordinates of the j^{th} pixel centre of the i^{th} boundary B_i , then we minimize the quantity

$$E_G = \sum_{i=1}^{N_B} \left(\sum_{j=1}^{N_i^P} (y_{j,i} - ax_{j,i} - b_i)^2 \right),$$

where N_B is the number of boundaries of the considered fragment and N_i^P is the number of pixels that constitute the i^{th} boundary. Minimization of E_G implies that all its partial derivatives with respect to a and b_i , $i = 1, \dots, N_B$, are equal to zero. The related calculations lead to:

$$b_i = \frac{1}{N_i^P} \sum_{j=1}^{N_i^P} y_{j,i} - a \left(\frac{1}{N_i^P} \sum_{j=1}^{N_i^P} x_{j,i} \right) = M_y^i - aM_x^i, \quad a = \frac{\sum_{i=1}^{N_B} M_y^i \sum_{j=1}^{N_i^P} x_{j,i} - \sum_{i=1}^{N_B} \sum_{j=1}^{N_i^P} x_{j,i} y_{j,i}}{\sum_{i=1}^{N_B} M_x^i \sum_{j=1}^{N_i^P} x_{j,i} - \sum_{i=1}^{N_B} \sum_{j=1}^{N_i^P} x_{j,i}^2}.$$

For easy reference, we will also use the name ‘‘fragment LS grid’’ for this class of parallel lines. Therefore, we define the width W_i of the i^{th} black stripe to be the distance of two parallel lines best fitting the boundaries of the stripe in hand.

2) Distribution of the widths of the black and blue stripes

First, we test the hypothesis that the width values W_i of the black stripes follow a normal distribution. In Fig. 2(a) the W_i histogram is shown, together with the best fitting normal distribution. Now, according to Kolmogorov, we sort W_i in ascending order and for each sorted value W_i^s , we compute the empirical cumulative distribution function $F(W_i^s) = \{\text{Proportion of black stripe widths such that } W_j^s \leq W_i^s\} = \frac{i}{N_{BS}}$. Moreover, we consider the theoretical cumulative distribution function of the normal distribution $\Phi(W_i^s)$ with mean value $\mu = 0.345$ cm and standard deviation $\sigma = 6.06 \cdot 10^{-2}$ cm, of the best fitting normal distribution. Loosely speaking, the Kolmogorov test states that if $F(W_i^s)$ and $\Phi(W_i^s)$ are adequately close for all the available samples W_i^s , then the hypothesis that the widths of the black stripes come from this normal distribution is acceptable. In a strict form, we test the hypothesis:

H_0 : W_i come from $N(\mu, \sigma)$, against the alternative

H_1 : W_i come from another distribution,

using the Kolmogorov-Smirnov criterion:

Let $D_0 = \max \left\{ \left| \Phi(W_i^s) - F(W_i^s) \right|, i = 1, \dots, N_{BS} \right\}$ and let D_{N_{BS}, a_c} be a constant depending on the number of samples N_{BS} and the level of significance a_c . Then, if $D_0 < D_{N_{BS}, a_c}$ holds, one can

accept hypothesis H_0 . Otherwise, hypothesis H_1 holds with significance level a_c . We would like to point out that for the relatively large number of available black stripe samples and for level of significance $a_c = 0.01$, D_{N_{BS}, a_c} is approximately given by $\frac{1.63}{\sqrt{N_{BS}}}$.

Application of this criterion to all $N_{BS} = 782$ available black stripes, led to the result $D_0 = 0.0274$, while clearly $D_0 < D_{N_{BS}, a_c}$ is satisfied. In an analogous manner, we have demonstrated that the widths of the blue stripes (see Fig. 2(b)) follow a normal distribution with $\mu^\gamma = 0.55$ cm, $\sigma^\gamma = 1.022 \cdot 10^{-1}$ cm. In the case of the blue stripes, $N_{GS} = 769$, $D_0 = 0.0353$ and $D_0 < D_{N_{GS}, a_c}$ holds.

B. Deciding if two BBS fragments match

At this point, we adopt the logical assumption that two BBS fragments belong to the same blue-black striped decorative element if two proper subsets of their parallel line grids match, as shown, for example, in Fig. 3. In order to verify this assumption, we take the following steps:

1) STEP 1

We rotate the two considered BBS fragments so that their LS grids are parallel. Notice that there are two rotation angles, differing by π , that align the two fragments' parallel line grids. In the case that the limits of the blue-black striped element are present in both fragments, the rotation angle compatible with these limits is chosen. Otherwise, in the subsequent analysis, the relative positions of the two fragments corresponding to both rotation angles are considered.

2) STEP 2

Suppose that the first fragment considered to be in the left position includes N_1 black and blue belts, while the second fragment includes N_2 stripes. Without any loss of generality, we may assume that the first line of the LS grid of each fragment is the one on the top of each fragment, as well as that the sequences of stripes in both fragments start from a belt of the same colour. Let the sequence of widths of the left fragment be $U_i, i = 1, 2, \dots, N_1$ and that of the right fragment be $V_j, j = 1, 2, \dots, N_2$. We stress that sequences U_i, V_j refer to both black and blue stripes, thus, for example, U_1 may be black, U_2 blue, U_3 black, U_4 blue, etc.

Subsequently, we perform continuous virtual translations of the right fragment downwards, each time comparing the widths of the corresponding black and blue stripes. In fact we define the

sequences:

$$\tilde{U}_i = \begin{cases} 0, & i \leq 0 \\ U_i, & 1 \leq i \leq N_1 \\ 0, & i \geq N_1 + 1 \end{cases} \text{ and } \tilde{V}_i = \begin{cases} 0, & i \leq 3 - N_2 \\ V_i, & 4 - N_2 \leq i \leq 3 \\ 0, & i \geq 4 \end{cases}$$

We would like to point out that sequence \tilde{V}_i is chosen so as to ensure that at least three stripes in each of the two considered fragments are compared in the first step of the subsequent process.

We also define two ‘‘mask-like’’ sequences:

$$L_i = \begin{cases} 0, & i \leq 0 \\ 1, & 1 \leq i \leq N_1 \\ 0, & i \geq N_1 + 1 \end{cases} \text{ and } M_i = \begin{cases} 0, & i \leq 3 - N_2 \\ 1, & 4 - N_2 \leq i \leq 3 \\ 0, & i \geq 4 \end{cases}$$

Next, we start by comparing the first three stripes of the left fragment with the last three stripes of the right fragment, namely we compare the sequences $\tilde{U}_i \cdot M_i$ and $\tilde{V}_i \cdot L_i$. Subsequently, we shift \tilde{V}_i and M_i by two, i.e. we define the sequence $\tilde{V}_i^1 = \tilde{V}_{i+2}$ and $M_i^1 = M_{i+2}$, and we compare the two sequences $\tilde{U}_i \cdot M_i^1$ and $\tilde{V}_i^1 \cdot L_i$. In other words, we compare the widths of the first five stripes of the left fragment with the five last of the right fragment. We proceed in this way shifting \tilde{V}_i and M_i by 2ℓ , and generating the shifted sequences \tilde{V}_i^ℓ and M_i^ℓ , each time comparing the sequences $\tilde{U}_i \cdot M_i^\ell$ and $\tilde{V}_i^\ell \cdot L_i$ (see Figs. 4(a) and 4(b)). The procedure stops when $2\ell > (N_1 + N_2 - 6)$, namely when the widths of the first three stripes of the right fragment have been compared with those of the last three stripes of corresponding colour of the left fragment.

3) STEP 3

According to the procedure described in STEP 2, we must compare the widths of k stripes each time, which is equivalent to comparing sequences $\tilde{U}_i \cdot M_i^\ell$ and $\tilde{V}_i^\ell \cdot L_i$. We stress that k_1 of these stripes are black and k_2 are blue, $k_1 + k_2 = k$. Now, let λ_i and ν_i , $i = 1, \dots, k_1$ be the widths of the black stripes to-be-compared, in the left and the right fragment respectively. Similarly, let γ_j and δ_j , $j = 1, \dots, k_2$ be the corresponding widths of blue stripes to be compared. We will momentarily assume that the two fragments are unrelated, which means that random variables λ_i, ν_i on one hand and γ_j, δ_j on the other, are stochastically independent. Then, we choose as a first measure of comparison the sum of squared differences:

$$\eta^\ell = \sum_{i=1}^{k_1} (\lambda_i - \nu_i)^2 + \sum_{j=1}^{k_2} (\gamma_j - \delta_j)^2$$

4) *STEP 4*

We associate with each value of the measure of comparison η^ℓ a probability that the corresponding sets of k stripes actually match. This probability will be estimated in the following step.

Next, we will determine the type of distribution the terms $\eta_1^\ell = \sum_{i=1}^{k_1} (\lambda_i - \nu_i)^2$, $\eta_2^\ell = \sum_{j=1}^{k_2} (\gamma_j - \delta_j)^2$ follow, for each ℓ . In fact, since $\lambda_i, \nu_i, i = 1, \dots, k_1$, come from the same population $N(\mu, \sigma)$, then the variables $\tilde{\lambda}_i = \frac{\lambda_i - \mu}{\sqrt{2}\sigma}$, $\tilde{\nu}_i = \frac{\nu_i - \mu}{\sqrt{2}\sigma}$ follow the normal distribution $N\left(0, \frac{1}{\sqrt{2}}\right)$. Moreover,

$(\tilde{\lambda}_i - \tilde{\nu}_i)$ comes from a normal distribution with mean value 0 and variance 1. But, since $(\tilde{\lambda}_i - \tilde{\nu}_i)$ follows $N(0, 1)$, then quantity $\sum_{i=1}^{k_1} (\tilde{\lambda}_i - \tilde{\nu}_i)^2$ follows a chi-square distribution with k_1 degrees of freedom.

Therefore, the statistical distribution of quantity η_1^ℓ is also known, since $\eta_1^\ell = \sum_{i=1}^{k_1} (\lambda_i - \nu_i)^2 = 2\sigma^2 \cdot \sum_{i=1}^{k_1} (\tilde{\lambda}_i - \tilde{\nu}_i)^2$

Similarly, since the blue stripe widths γ_j, δ_j of the two fragments come from the $N(\mu^\gamma, \sigma^\gamma)$ distribution, we define quantities $\tilde{\gamma}_j = \frac{\gamma_j - \mu^\gamma}{\sqrt{2}\sigma^\gamma}$, $\tilde{\delta}_j = \frac{\delta_j - \mu^\gamma}{\sqrt{2}\sigma^\gamma}$, which both follow $N\left(0, \frac{1}{\sqrt{2}}\right)$

distribution. Therefore, $\sum_{j=1}^{k_2} (\tilde{\gamma}_j - \tilde{\delta}_j)^2$ follows a chi-square distribution with k_2 degrees of freedom

and eventually the distribution of quantity $\eta_2^\ell = \sum_{j=1}^{k_2} (\gamma_j - \delta_j)^2 = 2(\sigma^\gamma)^2 \sum_{j=1}^{k_2} (\tilde{\gamma}_j - \tilde{\delta}_j)^2$ is also well defined.

Next, in order to estimate the distribution of quantity η^ℓ we will employ the following Lemma.

LEMMA

Let x and y be two independent random variables following chi-square distributions with k_1 and k_2 degrees of freedom respectively, whose probability density functions are, say, $g_1(x)$ and $g_2(y)$. Next, if a and β are positive real constants, we define the random variable $z = a \cdot x + \beta \cdot y$. Then, the cumulative distribution function $G_z(t)$ of z is given by:

$$G_z(t) = \int_0^{t/a} \int_0^{(t-ax)/\beta} g_1(x) \cdot g_2(y) dy dx$$

Proof. In a rather straightforward manner, we proceed by stating the definition of $G_z(t)$, namely $G_z(t) = P(z \leq t) \Leftrightarrow G_z(t) = P(a \cdot x + \beta \cdot y \leq t)$. Therefore, in the x - y plane we want to estimate the probability that z is found in the domain $D = \left\{ x \in [0, \frac{t}{a}], y \in [0, \frac{t-a \cdot x}{\beta}] \right\}$

Now, since x and y are independent random variables, their joint probability density function is $g(x, y) = g_1(x) \cdot g_2(y)$ and $G_z(t) = \iint_D g(x, y) dx dy = \iint_D g_1(x) g_2(y) dx dy =$

$$= \int_0^{t/a} \int_0^{(t-a \cdot x)/\beta} g_1(x) g_2(y) dy dx \quad \text{Q.E.D.}$$

An immediate consequence of the above Lemma and the previous analysis is that quantity

$\eta^\ell = \eta_1^\ell + \eta_2^\ell = \sum_{i=1}^{k_1} (\lambda_i - \nu_i)^2 + \sum_{j=1}^{k_2} (\gamma_j - \delta_j)^2$ has a cumulative distribution function

$$G_{\eta^\ell}(t) = \int_0^{t/(2\sigma^2)} \int_0^{(t-2\sigma^2 \eta_1^\ell)/(2(\sigma^2)^\ell)} \chi_{k_1}(\eta_1^\ell) \cdot \chi_{k_2}(\eta_2^\ell) d\eta_2^\ell d\eta_1^\ell \quad (\text{II.B.1})$$

where $\chi_{k_1}(\eta_1^\ell), \chi_{k_2}(\eta_2^\ell)$ are the probability density functions of the chi-square distributions with k_1 and k_2 degrees of freedom respectively.

5) *STEP 5:*

Now, it is logical to assume that the smaller the value of η , the greater the probability that the two fragments match at the specific position. Clearly, ideal matching occurs when $\eta^\ell = 0$, meaning that in this case all corresponding black and blue stripes have exactly the same width, i.e. $\lambda_i = \nu_i, i = 1, 2, \dots, k_1$, and $\gamma_j = \delta_j, j = 1, 2, \dots, k_2$. On the other hand, given a small value of η^ℓ , say t_0 , then the cumulative distribution function $G_{\eta^\ell}(t_0)$ gives the probability that two independent, not matching fragments furnish $\eta^\ell = t_0$ without actually matching at this point, in other words, accidentally. Therefore, it is quite logical to assume that $P_M^\eta(\ell) = 1 - G_{\eta^\ell}(t_0)$ gives the probability that these two fragments indeed match in this position and have generated this small value of η^ℓ due to statistical fluctuations of the blue-black stripe width.

Hence, we define the following criteria to decide if two fragments match in a certain position: First, for each value of ℓ that gives rise to a corresponding virtual shift of the right fragment, we compute quantities η_1^ℓ, η_2^ℓ and η^ℓ , as described above. Suppose that their values are τ_1^ℓ, τ_2^ℓ and τ^ℓ respectively. Subsequently, we compute the cumulative distribution function of η^ℓ at τ^ℓ , i.e. $G_{\eta^\ell}(\tau^\ell)$ via (II.B.1) and quantity $P_M^\eta(\ell) = 1 - G_{\eta^\ell}(\tau^\ell)$. We consider $P_M^\eta(\ell)$ a measure of matching of the two fragments in hand for the relative position determined by ℓ . Therefore, if for a certain value of ℓ , one obtains an essential maximum of $P_M^\eta(\ell)$ (see Fig 5(a)) and if $P_M^\eta(\ell)$ is greater than a reasonable confidence level, say α^M , then we accept that the two fragments match, when a shift of ℓ is performed in the right fragment.

Next, we define a second criterion, which, in a sense, balances out the contribution of the black and blue stripes' squared differences of widths. More specifically, we define

$$\zeta^\ell = \frac{\sum_{i=1}^{k_1} (\lambda_i - \nu_i)^2}{2\sigma^2} + \frac{\sum_{j=1}^{k_2} (\gamma_j - \delta_j)^2}{2(\sigma^\gamma)^2} \Leftrightarrow \zeta^\ell = \sum_{i=1}^{k_1} (\tilde{\lambda}_i - \tilde{\nu}_i)^2 + \sum_{j=1}^{k_2} (\tilde{\gamma}_j - \tilde{\delta}_j)^2$$

Once more, we compute the cumulative distribution function of ζ^ℓ at ρ^ℓ , i.e. $H_{\zeta^\ell}(\rho^\ell)$ via the Lemma in step 4, as well as the alternative matching probability $P_M^\zeta(\ell) = 1 - H_{\zeta^\ell}(\rho^\ell)$. The peak at the proper matching position is sharper, in this case, and its value is certain orders of magnitude greater than the one obtained via criterion 1 (Fig 5(b)). If we also take into consideration that this second criterion is much less sensitive to the BBS width's variation, we feel that this second criterion is considerably superior.

Application of both criteria led to the correct matching – placement of more than 25 pairs of BBS fragments, all verified by specialized personnel. We would like to point out, that the aforementioned statistical method could be applied to achieve correct placement of fragments depicting other repeated patterns of drawing.

III. MATCHING OF FRAGMENTS BASED ON EXHAUSTIVE CURVE FITTING ANALYSIS

Next, we have considered another class of wall-painting fragments, like the one shown in Figs. 6,7. As a consequence of the results presented in [19], the idea emerged among the authors that handcrafted stencils may have been used by the artist(s) to draw these complicated figures in order to ensure steady line. Moreover, we have examined the possibility that at least some of these stencils may have been constructed with the use of geometrical methods. Although such a method of construction required considerable novelty for the era, we have decided to test this conjecture by

means of the procedure that will be described below.

A. Determining a number of potential stencils

First, we have determined a set of geometric shapes, whose conception and construction are not, from an archaeological and historical point of view, a priori prohibitive for the era. Thus, for example, the conics (hyperbola, ellipse, parabola) can be constructed with the use of a ruler, a pair of compasses and/or other simple instruments. Although such a method of construction can be considered to be highly novel for the era and even for the classical ages, one cannot a priori exclude the possibility that a person or a group of persons had conceived and constructed these geometric figures in 1650 B.C.

Subsequently, we have chosen a set of wall-painting contour lines looking “suspicious” to have been drawn by means of a stencil. Using the methods of image segmentation referred to in Section II, we have obtained a sequence of pixels (x_i^ℓ, y_i^ℓ) , $i = 1, 2, \dots, N_\ell$, forming the contour of a specific line. These pixels can be described by the sequence of vectors \vec{r}_i^ℓ , $i = 1, 2, \dots, N_\ell$ starting at a reference center and pointing to each pixel center.

Suppose that one wants to test if the ℓ^{th} contour line \vec{r}_i^ℓ , $i = 1, 2, \dots, N_\ell$, is the successful result of an artist’s attempt to draw a geometrical prototype described by the parametric vector equation $\vec{r}^M(t | \Pi)$, where t is the independent variable, Π is the set of curve parameters and superscript M stands for model. For example, for the hyperbola polar parametric equation:

$$\vec{r}^M(t | \Pi) = (x_0 + a \cosh(t - t_0) \cos(\phi_0) - b \sinh(t - t_0) \sin(\phi_0)) \cdot \vec{i} + (y_0 + a \cdot \cosh(t - t_0) \sin(\phi_0) + b \sinh(t - t_0) \cos(\phi_0)) \cdot \vec{j}$$

where $t \in \mathbf{R}$ is the independent variable and $\Pi = \{x_0, y_0, a, b, \phi_0, t_0\}$ is the hyperbola set of parameters consisting of: the hyperbola center coordinates (x_0, y_0) , the hyperbola axes a, b , the probable rotation angle of the hyperbola ϕ_0 and t_0 is the starting point of the hyperbola independent variable domain.

Next, we compute the optimal set of parameters Π^O and the corresponding sequence of values of the independent variable t_i , $i = 1, 2, \dots, N_\ell$, so that $\vec{r}^M(t | \Pi^O)$ best fits \vec{r}_i^ℓ according to a chosen norm L; for example, one may use either $L_1 = \sum_{i=1}^{N_\ell} |\vec{r}_i^\ell - \vec{r}^M(t_i | \Pi)|$ or $L_2 = \sum_{i=1}^{N_\ell} (\vec{r}_i^\ell - \vec{r}^M(t_i | \Pi))^2$.

The algorithms applied to achieve this are the well-known conjugate gradient and/or the easier to implement Nelder – Mead method, starting from a tentative set of values of Π and letting Π

converge to Π^0 so that L is minimized. We would like to point out that the employed in both methods values t_i of the model curve's independent variable are each time computed by spotting the intersection of the line passing from (x_0, y_0) and the corresponding pixel (x_i^ℓ, y_i^ℓ) of the drawn contour line, on one hand, and the model curve on the other.

In order to verify that the specific contour line is best approximated by, say, a hyperbola, and not an ellipse or some other conic or spiral, we have applied the above procedure using the parametric equations corresponding to the ellipse, the parabola, the involute of a circle and the exponential spiral. Notice that the use of the parametric form of the conic equations manifested essentially better convergence properties than the employment of the general conic equation in Cartesian coordinates. For each contour line, the corresponding shape of the stencil that was chosen was the one which gave a minimum value of L resulting to a maximum distance of the theoretical curve from the contour line of less than 10^{-3} m.

Using the aforementioned methodology, we have found that a class of contour lines, like the one shown in Fig. 6, is optimally approximated by a hyperbola with $a=14.4$ cm and $b=20.12$ cm, with a corresponding mean and maximum distance of this hyperbola from the specific contour line of 0.4 mm and 0.9 mm, respectively. Notice that we have found more that 10 realizations of this prototype curve of length of between 12cm and 22.5cm, in six figures belonging to three different wall paintings.

B. Placement of two parts of a contour line in their proper position

In this section, we will employ the results of Section III(a) for correcting misplacement or deciding proper placement of neighbouring fragments, which, however, are separated by a considerable gap.

Indeed, consider the hyperbola introduced immediately above, which optimally fits the contour line representing the hunch in Fig 6. Consider, moreover, the two parts of a fragmented contour line representing the outline of the lady's right hand in Fig 7(a) and Fig 7(b); notice that part of the drawn right hand is missing. A method we have applied for properly placing the two fragmented sections of the right hand in question in the overall painting is described by the following steps:

a) We choose the hand section already attached to the main body of the painting, and check if it optimally fits one of the verified stencils.

b) If so, we place the verified stencil, e.g. the hyperbola, in the proper position.

c) We check if the other hand section fits the same hyperbola.

d) If so, we place this second part at the proper point in the already placed hyperbola.

In order to achieve the aforementioned steps, we employ the Method stated below:

Method:

1) Frequently, the n pixels of an arbitrary contour line, and in particular of each considered part of the hand that resulted from the segmentation method, are very dense and misplaced. As a consequence, it is very difficult to achieve one to one correspondence between these pixels and points of the potential stencil. To circumvent this difficulty, we choose N_ℓ pixels out of the n pixels of the considered contour line such that two successive selected pixels are separated by a small number of contour line pixels, say three or four. In the following, when we refer to the N_ℓ -pixel contour line of each part, we mean the aforementioned subset of the initial set of contour line pixels, consisting, say, of the set of points $a_1, a_2, \dots, a_{N_\ell}$.

We let d_j^P be the Euclidean distance between the j^{th} and the $j+1^{\text{th}}$ pixels of the contour line and $D(M, \Lambda)$ be the Euclidean distance between any two points M and Λ .

2) Consider an arbitrary potential stencil with independent variable t . Then, one creates a set of points belonging to the potential stencil, starting at t_0 and ending at t_e , that are as dense as possible. In other words, one first generates a sequence of points of the potential stencil $P^S(t_i)$, $t_i \in [t_0, t_e]$, such that two successive points have a very small distance, much smaller than the pixel dimensions.

3) For each point k of the sequence $P^S(t_i)$, one creates a N_ℓ -vertex polygonal line, starting at the point $P^S(t_k)$ in hand. The first vertex of this polygonal line is called M_1^k , and the subsequent vertices are computed as follows: The second vertex M_2^k is the point $P^S(t_{k,2})$, such that the distance of M_1^k and M_2^k , $D(M_1^k, M_2^k)$ is as close to the distance d_1^P as possible; similarly, we choose M_3^k so that $D(M_2^k, M_3^k) \cong d_2^P$ and so on, until the last point $M_{N_\ell}^k$ has been defined, so as $D(M_{N_\ell-1}^k, M_{N_\ell}^k) \cong d_{N_\ell-1}^P$.

4) Consider the two coplanar sets of points, $a_1, a_2, \dots, a_{N_\ell}$ with coordinates (x_i, y_i) , $i = 1, \dots, N_\ell$ on one hand, and $M_1^k, M_2^k, \dots, M_{N_\ell}^k$ with coordinates (p_i, q_i) , $i = 1, \dots, N_\ell$, on the other. Suppose that one wants to estimate the optimum rotation and parallel translation, so as to fit polygon (x_i, y_i) to polygon (p_i, q_i) in the Least Squares sense. In other words, one wants to estimate the proper angle of rotation θ and (x_0, y_0) so that, if

$$\begin{bmatrix} X_i \\ Y_i \end{bmatrix} = \begin{bmatrix} \cos(\theta) & -\sin(\theta) \\ \sin(\theta) & \cos(\theta) \end{bmatrix} \cdot \begin{bmatrix} x_i \\ y_i \end{bmatrix} + \begin{bmatrix} x_0 \\ y_0 \end{bmatrix}$$

then quantity

$$E_2 = \sum_{i=1}^{N_\ell} \left\{ (X_i - p_i)^2 + (Y_i - q_i)^2 \right\}$$

is minimized. Clearly, this requirement implies that

$$\frac{\partial E_2}{\partial x_0} = 0, \quad \frac{\partial E_2}{\partial y_0} = 0, \quad \frac{\partial E_2}{\partial \theta} = 0$$

After some straightforward calculus one obtains:

$$x_0 = \frac{1}{N_\ell} \sum_{i=1}^{N_\ell} (p_i - \delta x_i), \quad y_0 = \frac{1}{N_\ell} \sum_{i=1}^{N_\ell} (q_i - \delta y_i), \quad \tan(\theta) = \frac{\sum_{i=1}^{N_\ell} (x_i \delta q_i - y_i \delta p_i)}{\sum_{i=1}^{N_\ell} (x_i \delta p_i + y_i \delta q_i)}$$

where

$$\delta x_i = -y_i \sin(\theta) + x_i \cos(\theta), \quad \delta y_i = y_i \cos(\theta) + x_i \sin(\theta)$$

$$\delta p_i = \frac{1}{N_\ell} \sum_{j=1}^{N_\ell} p_j - p_i, \quad \delta q_i = \frac{1}{N_\ell} \sum_{j=1}^{N_\ell} q_j - q_i$$

Clearly, if we substitute these values of x_0, y_0, θ in E_2 , we obtain the corresponding minimum error $E_2^{\min}(k)$.

5) For all k , we apply the aforementioned step 4 and, therefore, for each point $P^S(t_k)$ of the specific potential stencil we obtain a minimum error $E_2^{\min}(k)$ describing the way the contour line of the considered part best fits the specific model poly-line at that point. Clearly, the minimization of $E_2^{\min}(k)$, for all points $P^S(t_k)$, for which the model poly-line can be constructed, offers the position, i.e. the value of k , at which the contour line in hand best fits the specific potential stencil. The corresponding minimum value of $E_2^{\min}(k)$ is a measure of the goodness of fit of these two sets of points.

6) In order to successfully position two candidate parts, say Π_1 and Π_2 , of a broken contour line in a figure, we first apply the five aforementioned steps on these two parts and in connection with the same stencil, and, in particular, the hyperbola determined in Section III(a). Suppose that this process confirms that both parts correspond to two different segments of the same considered stencil, which is placed at a reference position, as shown in Fig. 8. In other words, the first part fits the segment of the stencil, say SG_1 , starting at point k_1 and ending at point $k_1 + \ell_1$ with a minimum error $E_2^{\min}(k_1)$ smaller than a properly selected threshold, in particular $\alpha = 5 \cdot 10^{-4}$ m. This threshold value was

selected so as to obtain a closeness of fit between the contour line and the stencil similar to the one given by the hyperbola shown in Fig. 6. Similarly, the second part fits the segment of the same stencil, say SG_2 , starting at point k_2 and ending at point $k_2 + \ell_2$ with a corresponding error $E_2^{\min}(k_2) \leq \alpha$. We stress that the two model segments, SG_1 and SG_2 , must be disjoint. Let, moreover, (x_1, y_1) be the displacement and θ_1 the rotation angle computed with the application of step 4, so that part Π_1 optimally matches segment SG_1 of the stencil in its reference position, while (x_2, y_2) and θ_2 are the corresponding parameters for which Π_2 optimally fits SG_2 . Then, by rotating the model stencil by $-\theta_1$ and translating it by $(-x_1, -y_1)$ from its reference position, we optimally place the model stencil in hand on the wall-painting image, as shown in Fig. 9. In an analogous manner, by rotating part Π_2 by $\theta_2 - \theta_1$ and translating it by $(x_2 - x_1, y_2 - y_1)$ from its initial position, we place Π_2 optimally on the wall painting image, as shown in Fig 10.

We would like to emphasize that the aforementioned method is applicable independently of the shape of the stencil in hand. In fact, the authors have determined stencils corresponding to linear spirals [19]. Overall, they have applied the approach introduced here in matching at least 14 pairs of neighbouring fragments that were not in contact.

REFERENCES

- [1] C. Doulas, "The Wall-Paintings of Thera", The Thera Foundation, Petros Nomikos, Greece: Kapon Editions, 2nd ed., 1999
- [2] Michael Werman and Daniel Keren, "A Bayesian Method for Fitting Parametric and Nonparametric Models to Noisy Data", *IEEE Transactions on Pattern Analysis and Machine Intelligence*, vol. 23, no. 5, pp. 528 – 534, May 2001
- [3] Klaus Voss, Herbert Suesse, "Invariant Fitting of Planar Objects by Primitives", *IEEE Transactions on Pattern Analysis and Machine Intelligence*, vol. 19, no. 1, pp. 80-84, January 1997
- [4] N. Chernov, C. Lesort "Statistical efficiency of curve fitting algorithms", *Computational Statistics & Data Analysis*, vol. 47, no 4, pp. 713-728, November 2004
- [5] Kanatani, K., "Statistical bias of conic fitting and renormalization", *IEEE Transactions on Pattern Analysis and Machine Intelligence*, pp. 320 – 326, March 1994
- [6] A. Atieg G. A. Watson, "A class of methods for fitting a curve or surface to data by minimizing the sum of squares of orthogonal distances", *Journal of Computational and Applied Mathematics*, vol. 158, no 2), pp. 277-296, September 2003
- [7] Hung-Hsin Chang and Hong Yan, "Vectorization of hand-drawn image using piecewise cubic Bezier curves fitting", *Pattern Recognition* 31, pp. 1747-1755, November 1998

- [8] Anil K. Jain, Robert P. W. Duin, Jianchang Mao, “Statistical Pattern Recognition: A Review”, *IEEE Transactions on Pattern Analysis and Machine Intelligence*, vol. 22, no 1, pp. 4 – 37, January 2000
- [9] Joseph, E. Pavlidis, T, “Bar code waveform recognition using peak locations”, *IEEE Transactions on Pattern Analysis and Machine Intelligence*, vol. 16, no 6, pp. 630 – 640, June 1994
- [10] C. Papaodysseus, Th. Panagopoulos, M. Exarhos, C. Triantafyllou, D. Fragoulis, “Contour-shape Based Reconstruction of Fragmented, 1600 B.C. Wall Paintings”, *IEEE Transactions on Signal Processing*, vol. 50, no 6, pp.1277-1288, June 2002.
- [11] Cooper D. B., Willis A., Andrews S., Baker J., Cao Y., Han D., Kang K., Kong W., Leymarie F. F., Orriols X., Velipasalar S., Vote E. L., Joukowsky M. S., Kimia B. B., Laidlaw D. H., Mumford D, “Assembling virtual pots from 3d measurements of their fragments”. *Proceedings of the 2001 conference on Virtual reality, archeology, and cultural heritage (2001)*, ACM Press, pp. 241-254.
- [12] Kong W., Kimia B.B., “On solving 2D and 3D puzzles using curve matching”. *IEEE Computer Society Conference on Computer Vision and Pattern Recognition (CVPR �01)*, vol. 2, pages 583-590, 2001.
- [13] Leityo H.C.G., Stolfi J., “A multi-scale method for the re-assembly of twodimensional fragmented objects”. *IEEE Transactions of Pattern Analysis and Machine Intelligence*, 24(9), 2002, pp. 1239-1251.
- [14] Papaioannou G., Karabassi E., and Theoharis T., “Virtual archaeologist: Assembling the past”, *IEEE Computer Graphics*, 21(2):53-59, March-April 2001.
- [15] T. Gevers and A. W. M. Smeulders, “Combining region splitting and edge detection through guided Delaunay image subdivision”, *IEEE Computer Vision and Pattern Recognition*, pp. 1021-1026, 1997
- [16] Stan Z. Li, “Toward global solution to MAP image restoration and segmentation: using common structure of local minima”, *Pattern Recognition* 33, pp. 715-723, April 2000
- [17] Ramón Román-Roldán, Juan Francisco Gómez-Lopera, Chakir Atae-Allah, José Martínez-Aroza and Pedro Luis Luque-Escamilla, “A measure of quality for evaluating methods of segmentation and edge detection”, *Pattern Recognition* 34, pp. 969-980, May 2001
- [18] Th. Panagopoulos, C. Papaodysseus, M. Exarhos, C. Triantafillou, G. Roussopoulos, P. Roussopoulos, “Prehistoric Wall-Paintings Reconstruction Using Image Pattern Analysis And Curve Fitting”, *WSEAS Transactions on Electronics*, vol. 1, no 1, pp. 108-113, January 2004
- [19] C. Papaodysseus, M. Exarhos, Th. Panagopoulos, C. Triantafillou, George Roussopoulos, A. Pantazi, V. Loumos, D. Fragoulis, Chr. Doulmas, “Identification of Geometrical Shapes in Paintings and its Application to Demonstrate the Foundations of Geometry in

1650 B.C.”, *IEEE Transactions on Image Processing*, vol. 14, no 7, pp. 862-873, July 2005.



Fig. 1. A typical set of fragments depicting alternating black and blue stripes.

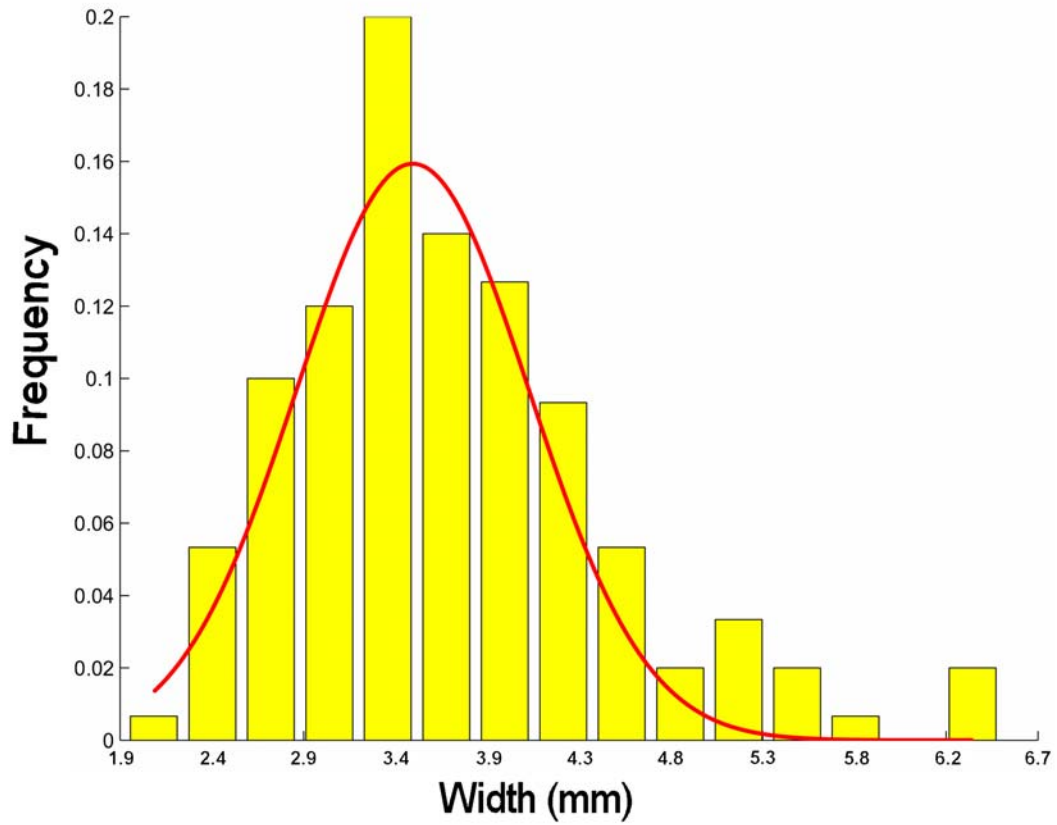


Fig. 2(a). The black stripe width W_i histogram, together with the best fitting normal distribution. For the black stripe width population, $\mu = 0.345$ cm, $\sigma = 6.06 \cdot 10^{-2}$ cm, $N_{BS} = 782$

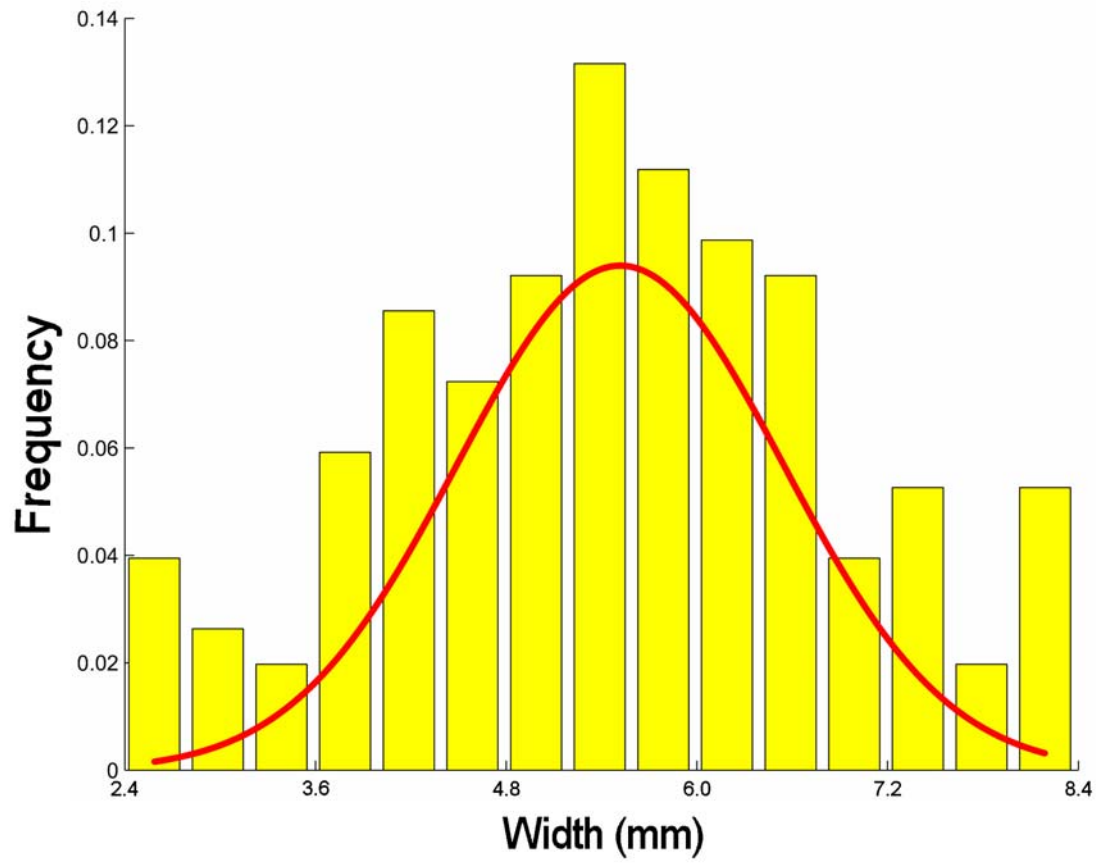


Fig. 2(b). The blue stripe width histogram, together with the best fitting normal distribution. For the blue stripe width population, $\mu^\gamma = 0.55$ cm, $\sigma^\gamma = 1.022 \cdot 10^{-1}$ cm, $N_{GS} = 769$

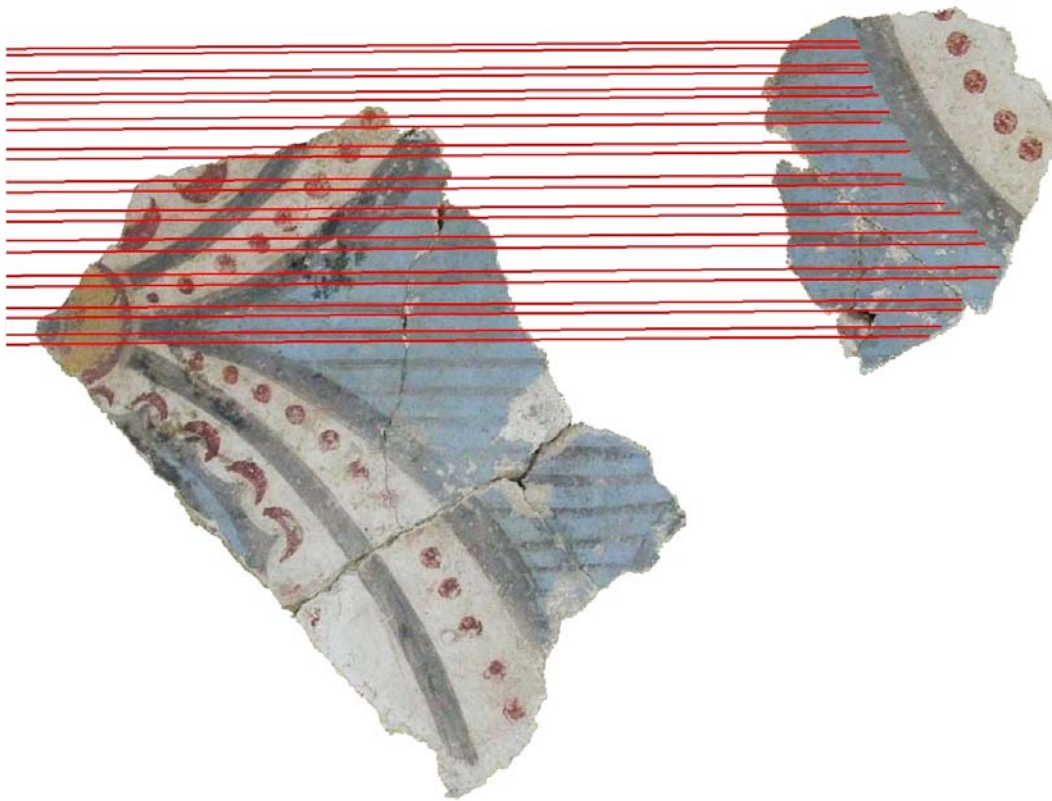


Fig. 3. Two fragments that have been found to statistically match.

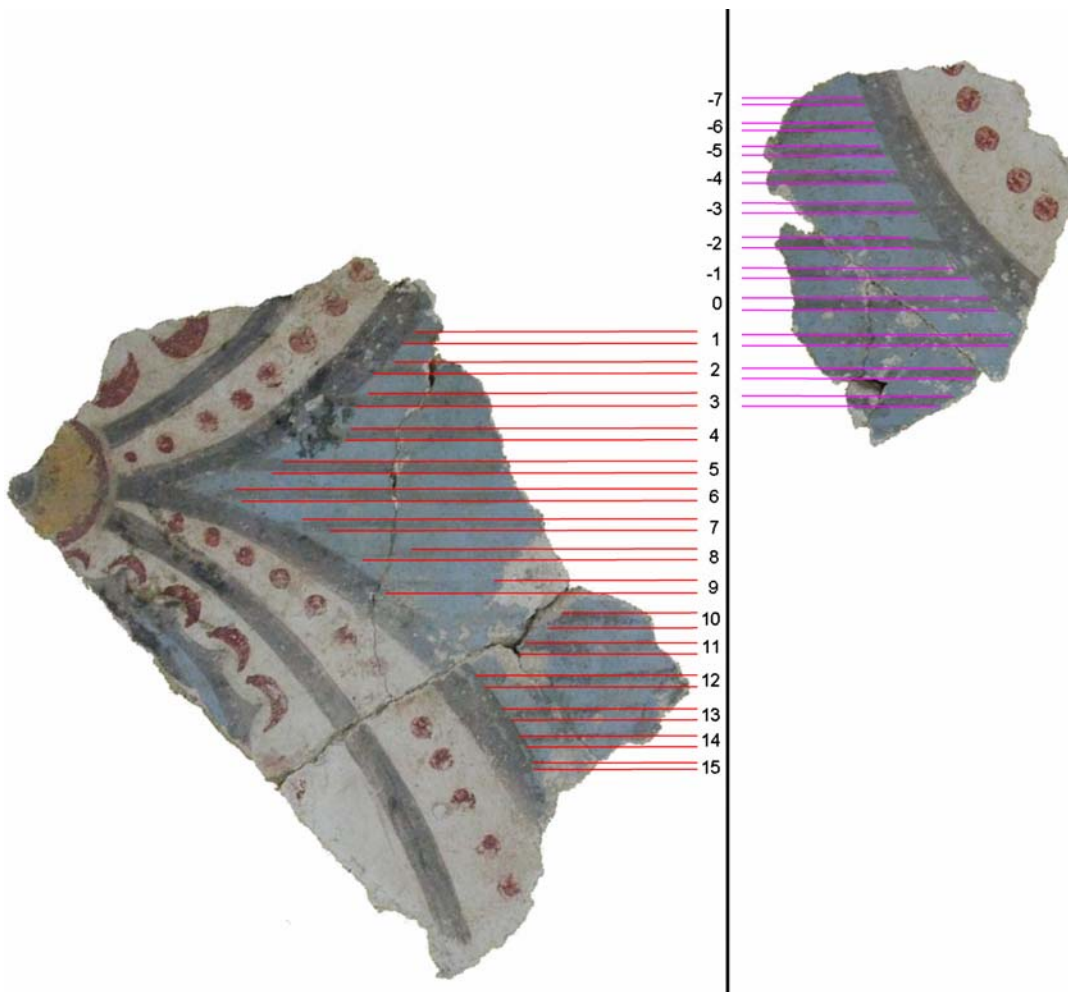


Fig 4(a). Two stages of the stripe widths' comparison process.

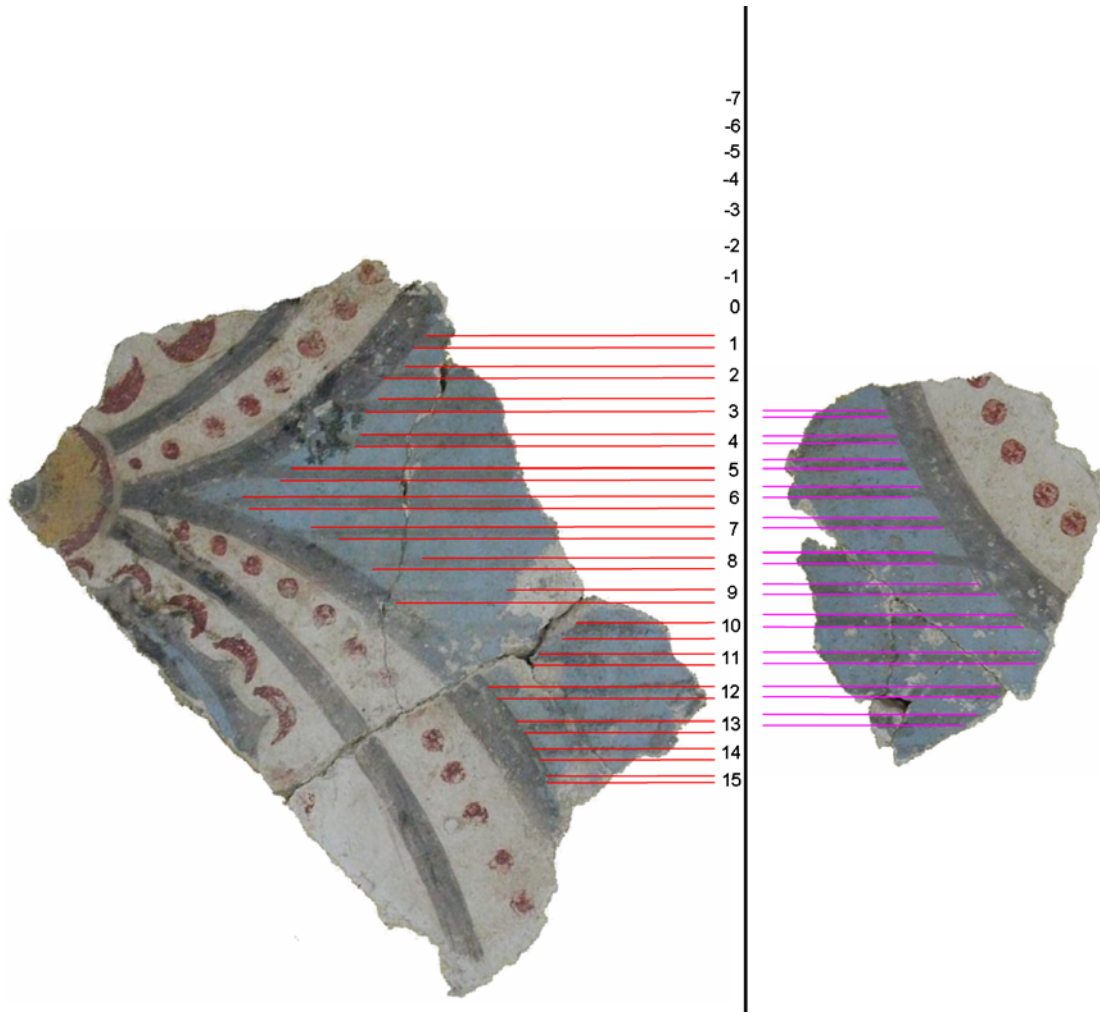


Fig. 4(b). Two stages of the stripe widths' comparison process.

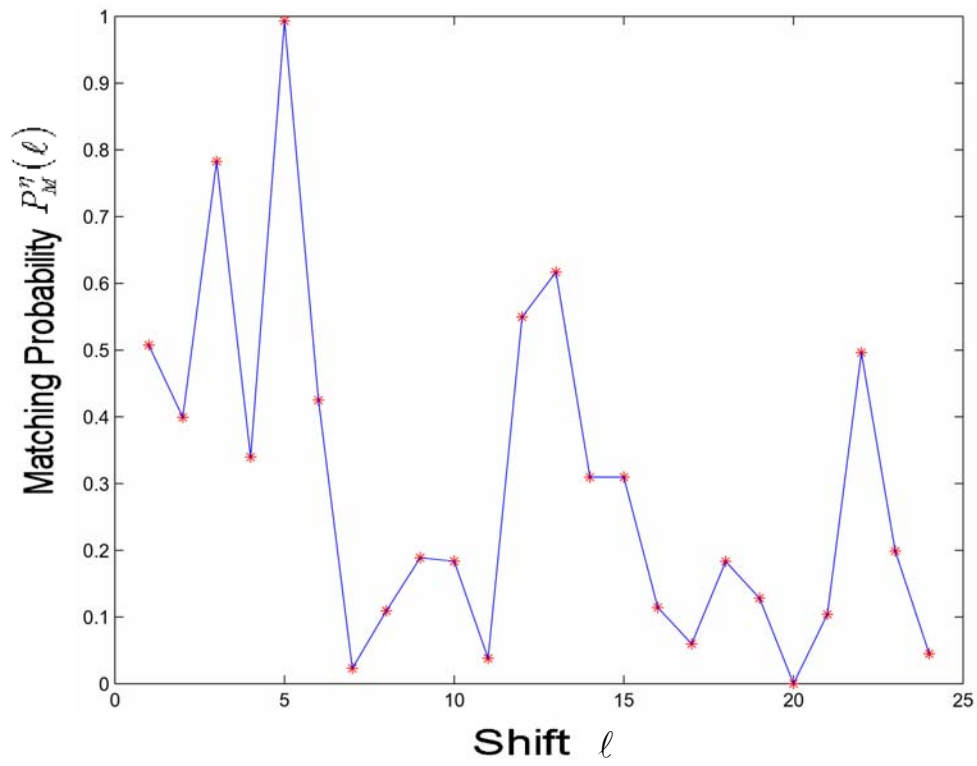


Fig 5(a). The values of $P_M^n(\ell)$ obtained with the use of the first criterion. At the optimal position, $P_M^n(5) = 0.993109$

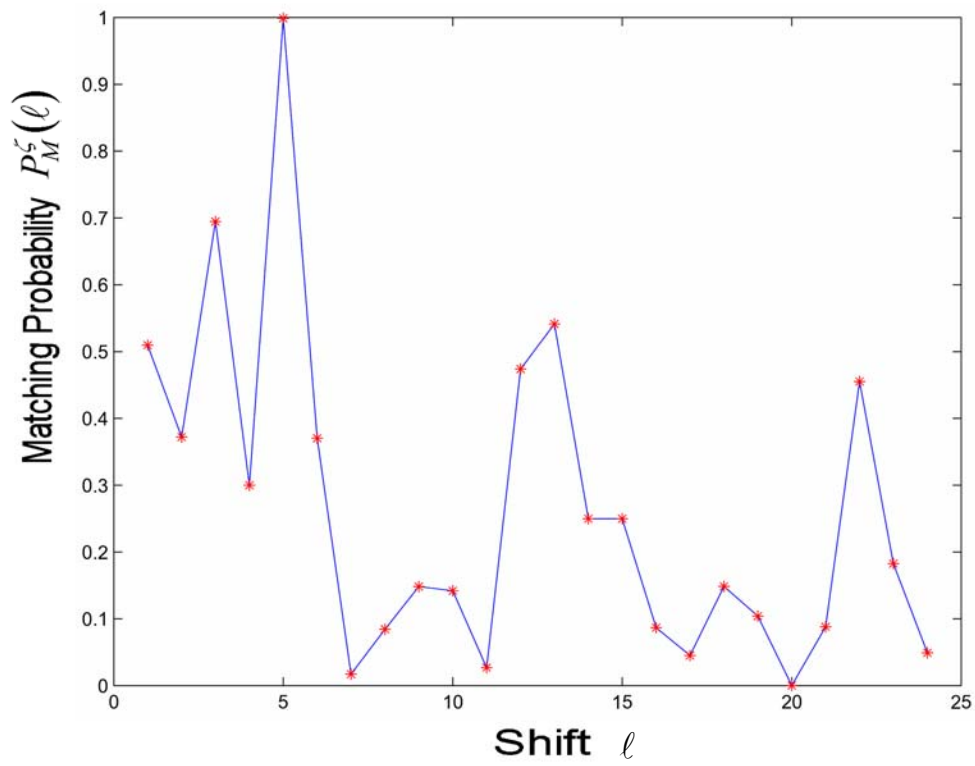


Fig.1 5(b). The values of $P_M^zeta(\ell)$ obtained with the use of the second criterion. At the optimal matching position, $P_M^zeta(5) = 0.999626$



Fig. 6. Example of the hyperbola that optimally approximates the contour line that represents the hunch of the female figure.



Fig 7(a). The unplaced fragment of the wall painting, which contains part of the wrist of the lady's hand. (Not to scale)



Fig 7(b). The wall painting section that contains the body and part of the arm of the lady.

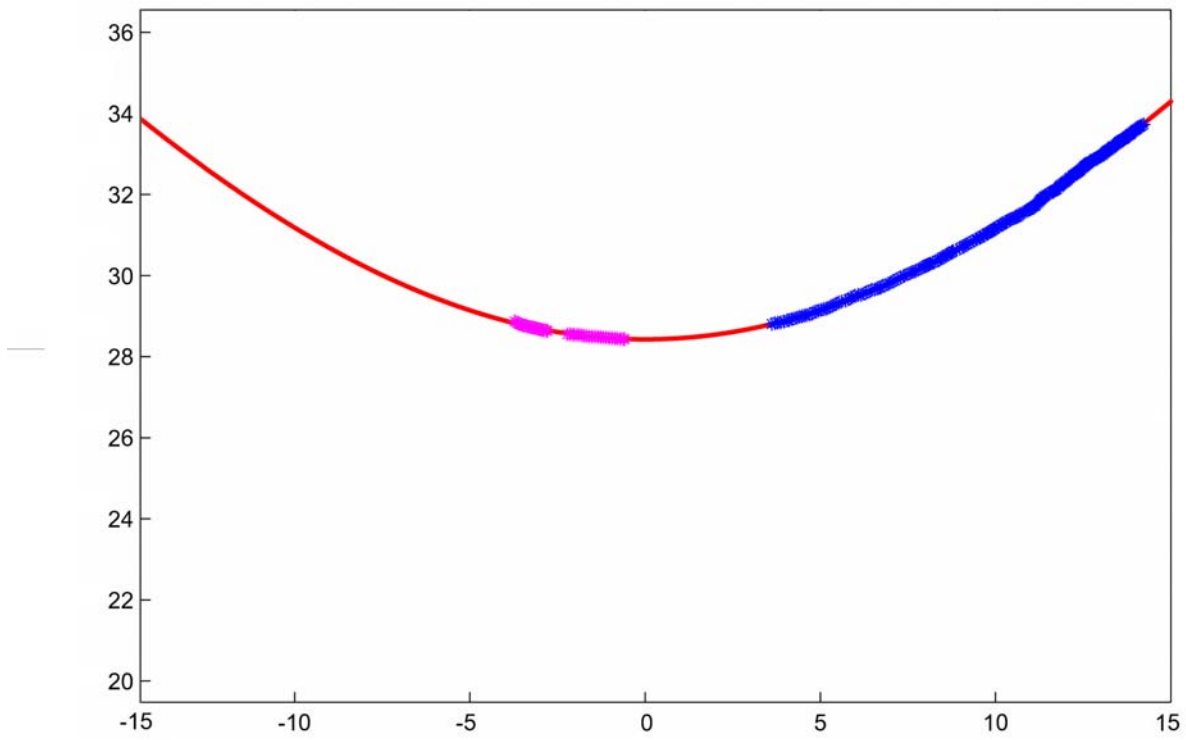


Fig. 8. The hyperbola in its reference position, with the two contour lines optimally placed on it.

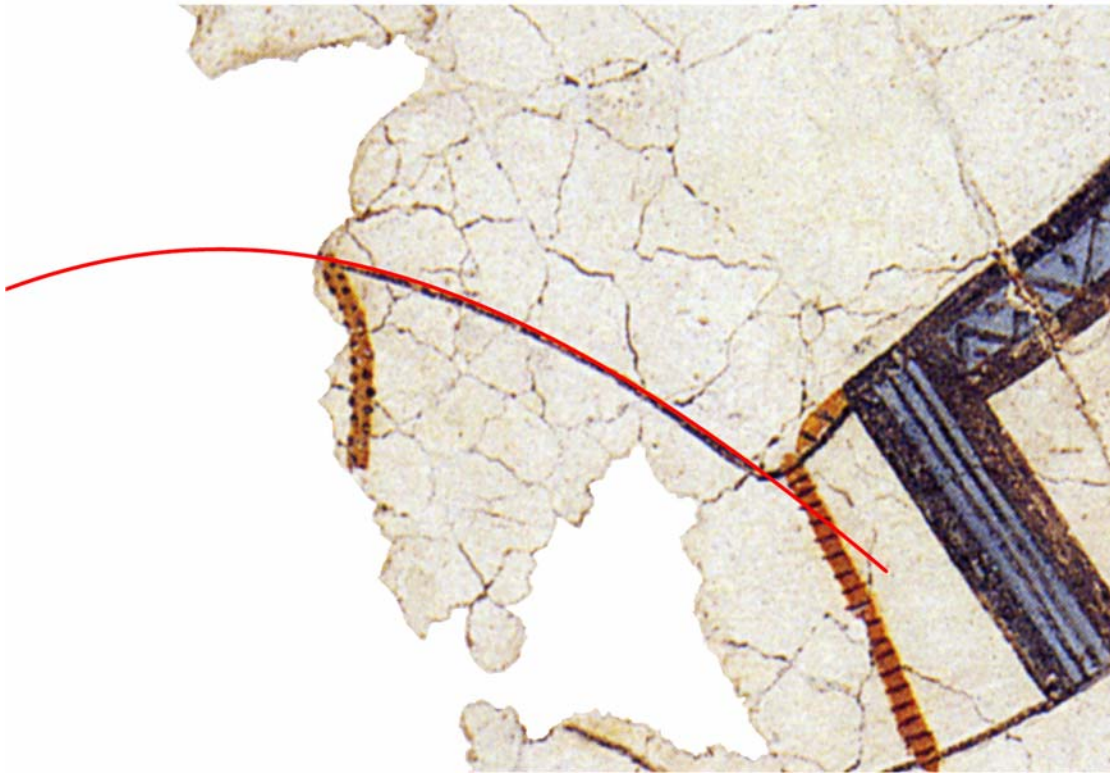


Fig. 9. The outstretched arm with the optimally fitting hyperbola superimposed on it.

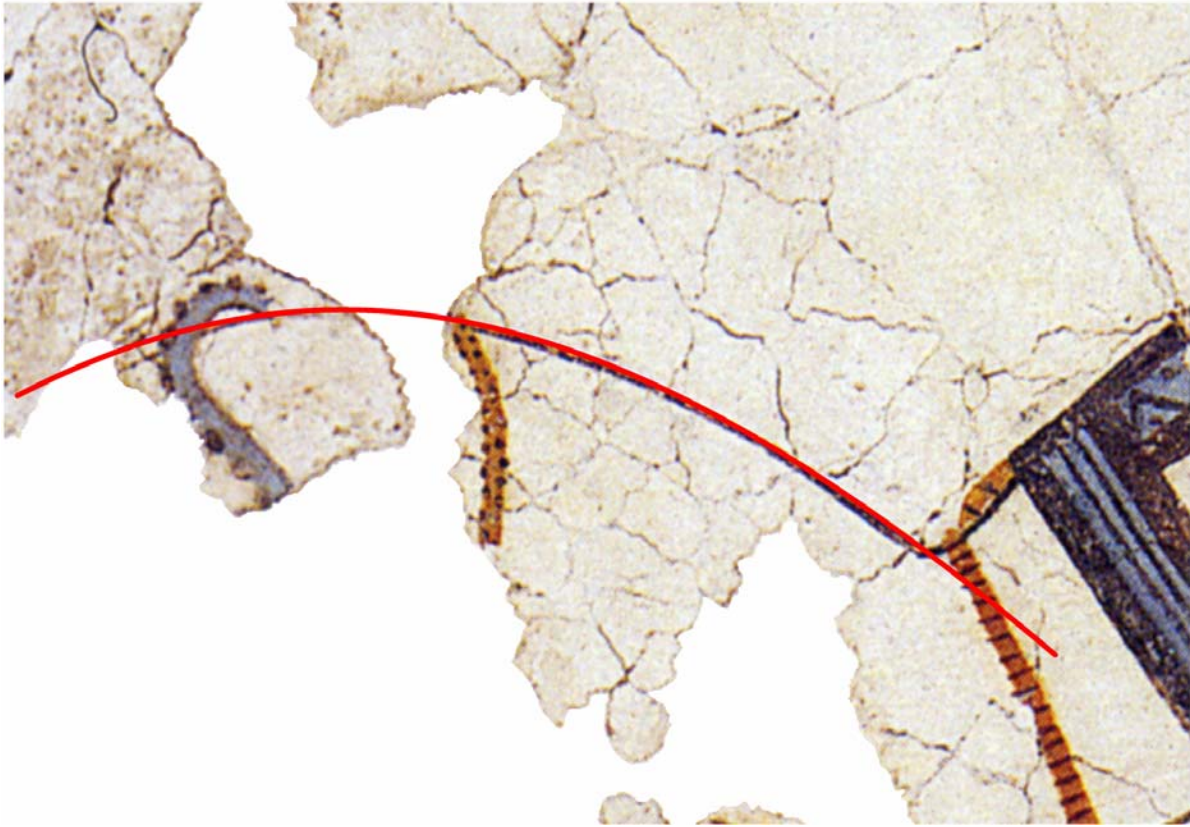


Fig. 10. Final placement of the wrist fragment with the use of the hyperbola.